scientific reports

Check for updates

OPEN

# First independent validation of the proton-boron capture therapy concept

Anna Jelínek Michaelidesová[1,2,5], Pavel Kundrát[1,5], Oldřich Zahradníček[1], Irina Danilová[1,2], Kateřina Pachnerová Brabcová[1], Jana Vachelová[1], Jan Vilimovský[3], Miroslav David[4], Vladimír Vondráček[3,4] & Marie Davídková[1]✉

**Boron has been suggested to enhance the biological effectiveness of proton beams in the Bragg peak region via the p + $^{11}$B → 3α nuclear capture reaction. However, a number of groups have observed no such enhancement in vitro or questioned its proposed mechanism recently. To help elucidate this phenomenon, we irradiated DU145 prostate cancer or U-87 MG glioblastoma cells by clinical 190 MeV proton beams in plateau or Bragg peak regions with or without $^{10}$B or $^{11}$B isotopes added as sodium mercaptododecaborate (BSH). The results demonstrate that $^{11}$B but not $^{10}$B or other components of the BSH molecule enhance cell killing by proton beams. The enhancement occurs selectively in the Bragg peak region, is present for boron concentrations as low as 40 ppm, and is not due to secondary neutrons. The enhancement is likely initiated by proton-boron capture reactions producing three alpha particles, which are rare events occurring in a few cells only, and their effects are amplified by intercellular communication to a population-level response. The observed up to 2–3-fold reductions in survival levels upon the presence of boron for the studied prostate cancer or glioblastoma cells suggest promising clinical applications for these tumour types.**

**Keywords** Proton radiotherapy, Proton-boron capture therapy, Sodium mercaptododecaborate (BSH), Biological effectiveness, Cell survival

Despite ongoing progress in early diagnosis as well as in treatment methods, cancer represents the second most frequent cause of deaths in developed countries. For most cancer patients, their treatment involves radiotherapy, either alone or in combination with surgery or chemotherapy. Conventional radiotherapy is based on the use of photon beams which after an initial build-up lead to dose profiles exponentially decreasing with increasing penetration depth. Side effects from inevitable irradiation of healthy tissues surrounding the tumour frequently limit the applicable dose and hence cure rates. On the other hand, heavy charged particles such as protons or heavier ions possess an inversed dose profile, depositing most energy in the so-called Bragg peak just before their stopping. Consequently, proton radiotherapy offers highly conformal dose distributions which deliver high dose to the tumour and largely spare surrounding healthy tissues and organs at risk. Paediatric patients or those with head-and-neck tumours are among those for whom the largest benefits from proton radiotherapy are expected[1].

A few years ago the idea of proton-boron capture therapy (PBCT) was proposed[2,3] as a strategy to amplify the benefits of proton therapy. PBCT can be viewed as a modality combining the concepts of proton radiotherapy and boron-neutron capture therapy (BNCT). It utilizes the proton-boron nuclear capture reaction, p + $^{11}$B → 3α. The produced alpha particles possess a short range in tissue and represent a densely ionizing type of radiation, i.e. provide a very localized and highly effective irradiation, similarly to the $^{10}$B + n → α + $^{7}$Li reaction that underpins BNCT[4]. Contrary to sparsely available and hardly focusable neutron beams required for BNCT, PBCT combines the ballistic precision of proton irradiation with the localized and highly effective nature of the alpha component and offers prospects for the treatment of hypoxic or radioresistant tumours[3]. Effectively enhancing the proton dose and its conformity to the tumour, PBCT would also help reduce proton therapy costs by reducing the number of fractions needed and increasing patient throughput.

[1]Nuclear Physics Institute of the Czech Academy of Sciences, Husinec - Řež 130, 250 68 Řež, Czech Republic. [2]Faculty of Nuclear Sciences and Physical Engineering, Czech Technical University in Prague, Břehová 78/7, 115 19 Prague, Czech Republic. [3]Proton Therapy Center Czech, Prague, Budínova 2437/1a, 180 00 Prague, Czech Republic. [4]Thomayer University Hospital, Vídeňská 800, 140 59 Prague, Czech Republic. [5]These authors contributed equally: Anna Jelínek Michaelidesová and Pavel Kundrát. ✉email: davidkova@ujf.cas.cz

The effectiveness of PBCT has recently been demonstrated in pioneering experiments[3,5,6]. In these in vitro studies, the authors reported boron-mediated enhanced effectiveness in killing DU145 prostate and PANC-1 pancreatic cancer cells as well as in inducing chromosome aberrations in breast epithelial MCF-10A cells. They used proton beams of energies ranging from 1 to 165 MeV and boron concentrations of 40 or 80 ppm of $^{11}$B in the form of sodium mercaptododecaborate (BSH), a compound widely used and concentrations reached in BNCT applications[4,7,8]. Originally, PBCT was thought to result in dose enhancement of the order of 50–100% via the produced alpha particles, leading to increased biological effects[2,9]. However, later studies[10–12] pointed out that under clinically relevant boron concentrations, this alpha-related dose is several orders of magnitude smaller than the dose from the proton beams and thus virtually negligible, questioning the mechanisms proposed to underpin PBCT. A potential role for secondary neutrons captured by $^{10}$B in PBCT was suggested[13]. Furthermore, a number of experimental studies have been published recently[14–16] that provide negative or inconclusive data on PBCT effectiveness.

To help address the validity and generality of PBCT, in this work we independently tested PBCT effectiveness for DU145 cells originally used in the pioneering PBCT experiments[3,5,6] and expanded the tests for U-87 MG glioblastoma cells. The results provide the first independent validation of PBCT and demonstrate its validity for U-87 MG glioblastoma. Further, we performed dedicated experiments to help elucidate PBCT mechanisms, in particular to test the potential role of secondary neutrons captured by $^{10}$B suggested as an alternative to p + $^{11}$B capture[13]. We alternatively used $^{nat}$BSH, i.e. BSH with the natural isotopic ratio of boron ($^{nat}$B containing 80% $^{11}$B and 20% $^{10}$B), or $^{10}$BSH, i.e. BSH with highly enhanced content of $^{10}$B (virtually 100% $^{10}$B). As an independent benchmark on the role of neutrons in PBCT, we irradiated the U-87 MG cells with clinical 6 and 18 MV photon beams, the latter including and the former virtually absent of secondary neutrons. The results do not suggest an important role of secondary neutrons.

## Results

### Independent validation of PBCT in DU145 cells

To verify the PBCT concept, we first irradiated DU145 prostate cancer cells, the cell line for which the PBCT was observed originally[3,5,6]. The cells were irradiated by monoenergetic 190.6 MeV proton beams (range in water of 23.9 cm) in plateau (entrance) or Bragg peak positions (2.1 and 23.6 cm water-equivalent depths, respectively). Cells were irradiated in the absence or presence of $^{nat}$BSH at 40 ppm $^{nat}$B (32 ppm $^{11}$B), a concentration within ranges reached in clinical BNCT applications[4,7,8]. Cell survival fractions were obtained via the standard colony formation assay, scoring colonies of at least 50 cells 12 days post irradiation. Comparing plating efficiencies in unirradiated samples with and without boron, 0.303 ± 0.061 vs 0.341 ± 0.057 mean values and standard deviations from n = 4 independent experiments, revealed no signs of boron toxicity in terms of cell killing, in agreement with the experience from BNCT applications. As shown in Fig. 1, the presence of $^{nat}$BSH did not modulate the survival of DU145 cells in the plateau region (blue squares). Cell survival in the Bragg peak region (empty red triangles) was notably reduced compared to the plateau region. It was further reduced upon the presence of $^{nat}$BSH (filled red triangles), by factors of 2–3 at the highest studied doses. The measured data were fitted by the classical linear-quadratic (LQ) model of cell survival, $SF = \exp(-\alpha D - \beta D^2)$; the fits are included in Fig. 1 (lines),

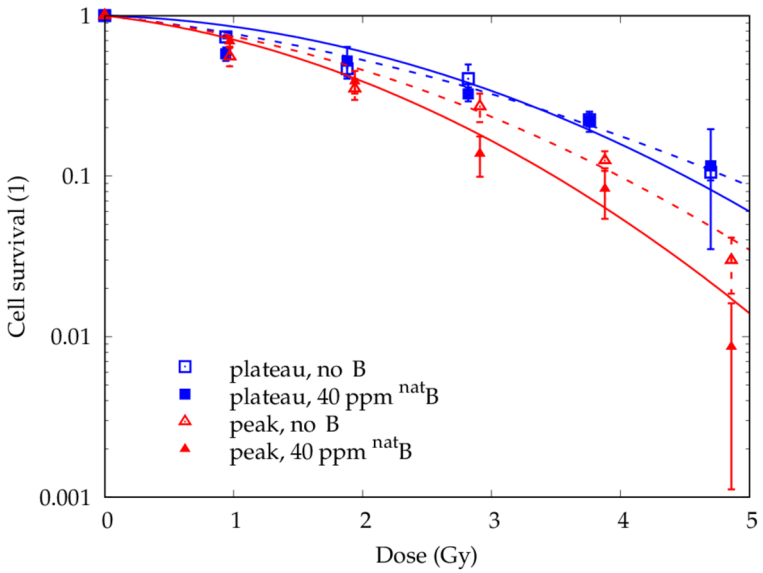


**Figure 1.** Survival of DU145 prostate cancer cells following irradiation by 190.6 MeV proton beams in plateau or peak regions without or with the presence of $^{nat}$BSH at a concentration of 40 ppm $^{nat}$B (i.e., 32 ppm $^{11}$B). Points represent mean values from at least 2 independent experiments, error bars depict standard errors of the mean, and lines show the corresponding LQ fits.

and the corresponding model coefficients are listed in Table 1. Due to biological variabilities and the low number of independent experiments (in particular at the highest dose), the data and consequently the reported LQ coefficients possess large uncertainties, and the observed boron enhancement did not reach statistical significance ($p = 0.125$). Yet, these results provided a preliminary validation of the PBCT concept.

## PBCT in U-87 MG cells

To further test the PBCT concept, its generality and potential underpinning mechanisms, we measured the survival of U-87 MG glioblastoma cells irradiated using the same proton beams and positions as described above, with the absence or presence of 40 ppm $^{nat}$B or $^{10}$B in the form of BSH. There were no signs of boron toxicity to U-87 MG cells at the applied concentration (plating efficiencies in unirradiated samples of $0.189 \pm 0.049$ without vs $0.196 \pm 0.059$ with $^{nat}$BSH, from n = 7 independent experiments; $0.271 \pm 0.021$ without vs $0.254 \pm 0.058$ with $^{10}$BSH, n = 2). As depicted in Fig. 2a, the presence of BSH did not modify the killing of U-87 MG cells by the proton beam in the plateau position, either with the natural isotopic mixture of boron or with $^{10}$B. Irradiation in the Bragg peak position (Fig. 2b) was more effective in killing the cells than in the plateau region. Cell survival was slightly reduced upon the presence of $^{10}$BSH (not reaching statistical significance, $p = 0.067$), and notably reduced by $^{nat}$BSH (highly statistically significant, $p = 2 \times 10^{-5}$), by a factor of about 2 at the highest doses. The data were fitted by the LQ model (lines); the resulting coefficients are listed in Table 2.

These results support the concept of PBCT and demonstrate its validity for U-87 MG glioblastoma cells, at proton energy as high as 190 MeV and boron levels of 40 ppm $^{nat}$B ($^{11}$B of 32 ppm) only. Furthermore, the results demonstrate that the key player involved in the observed effects is $^{11}$B likely capturing protons, and not $^{10}$B capturing secondary neutrons or another component of the BSH molecule such as the thiol (SH) group.

To additionally assess the potential role of thermal neutron capture by $^{10}$B, we compared killing of U-87 MG cells by therapeutic 6 and 18 MV photon beams. This was motivated by the well-known fact that while secondary neutrons are abundant in 18 MV beams, they are virtually absent in 6 MV beams for which the photon energies are below the threshold for photoneutron production reactions[17]. Thus, if the observed boron-mediated enhancements of proton effects were due to n + $^{10}$B capture rather than due to p + $^{11}$B, similar enhancements should be present also for 18 MV photons, but not for 6 MV ones. Despite some variability typical for radiobiological experiments, the results presented in Fig. 3 do not reveal any statistically significant differences between 6 or 18 MV beams without BSH or with $^{nat}$BSH or $^{10}$BSH ($p > 0.14$ for all pairwise comparisons). The LQ model coefficients are listed in Table 3. In agreement with the aforementioned data, these results point against the potential key contribution of secondary neutrons in the observed PBCT in U-87 MG cells.

## Dose-modifying factor

To capture the magnitude of PBCT effects, a dose-modifying factor (DMF) was introduced[3], defined as the ratio of doses without and with the presence of boron that produce a given effect, e.g. 10% cell survival, $DMF_{10\%}$. For the present data, the $DMF_{10\%}$ calculated from their LQ fits amounts to $1.14 \pm 0.34$ for DU145 cells and to $1.18 \pm 0.08$ for U-87 MG cells, respectively, for the Bragg peak position and with 40 ppm $^{nat}$B (32 ppm $^{11}$B); the reported uncertainties in DMFs refer to standard deviations. In other words, in the presence of 40 ppm $^{nat}$B, cell killing by protons in the Bragg peak increases as if the applied dose increased by 14% for DU145 and 18% for U-87 MG cells, respectively.

In Fig. 4, these results are compared with the data from the pioneering PBCT experiments[3,5,6]. DMFs generally decrease towards unity with increasing proton energy. DMFs at distal edges of spread-out Bragg peaks (SOBPs) are comparable to those from monoenergetic beams, as only protons started with the highest energy are present in distal SOBPs. DMF at mid-SOBPs (empty symbols) are smaller than at their distal edges, since the beam at the mid-SOBP position contains not only protons stopping there but also ones with higher energies and penetration depths, which are less effectively captured by $^{11}$B. As expected, DMFs decrease with decreasing $^{11}$B concentration. A comparison of DMFs for DU145 prostate and PANC-1 pancreatic cancer cells illustrates the biological variability between cell lines. The present results for DU145 and U-87 MG cells in the Bragg peak position of 190 MeV protons are in line with the previously published DMF values and these trends.

## Discussion

We have verified that the presence of $^{11}$B enhances cell killing by proton beams. For the DU145 prostate cancer cell line originally used in the pioneering PBCT experiments[3,5,6], statistical significance was not reached ($p = 0.125$), in particular due to only n = 2 independent experiments at the highest dose. For the U-87 MG

| Position | Boron presence | α ($Gy^{-1}$) | β ($Gy^{-2}$) |
|---|---|---|---|
| Plateau | None | $0.204 \pm 0.098$ | $0.057 \pm 0.021$ |
| | $^{nat}$B | $0.057 \pm 0.234$ | $0.101 \pm 0.049$ |
| Peak | None | $0.202 \pm 0.168$ | $0.094 \pm 0.036$ |
| | $^{nat}$B | $0.218 \pm 0.224$ | $0.127 \pm 0.047$ |

**Table 1.** Coefficients α and β of the LQ fit to survival data for DU145 cells irradiated by 190.6 MeV protons under the absence or presence of $^{nat}$BSH (40 ppm $^{nat}$B corresponding to 32 ppm $^{11}$B and 8 ppm $^{10}$B). Uncertainties are reported as standard deviations.

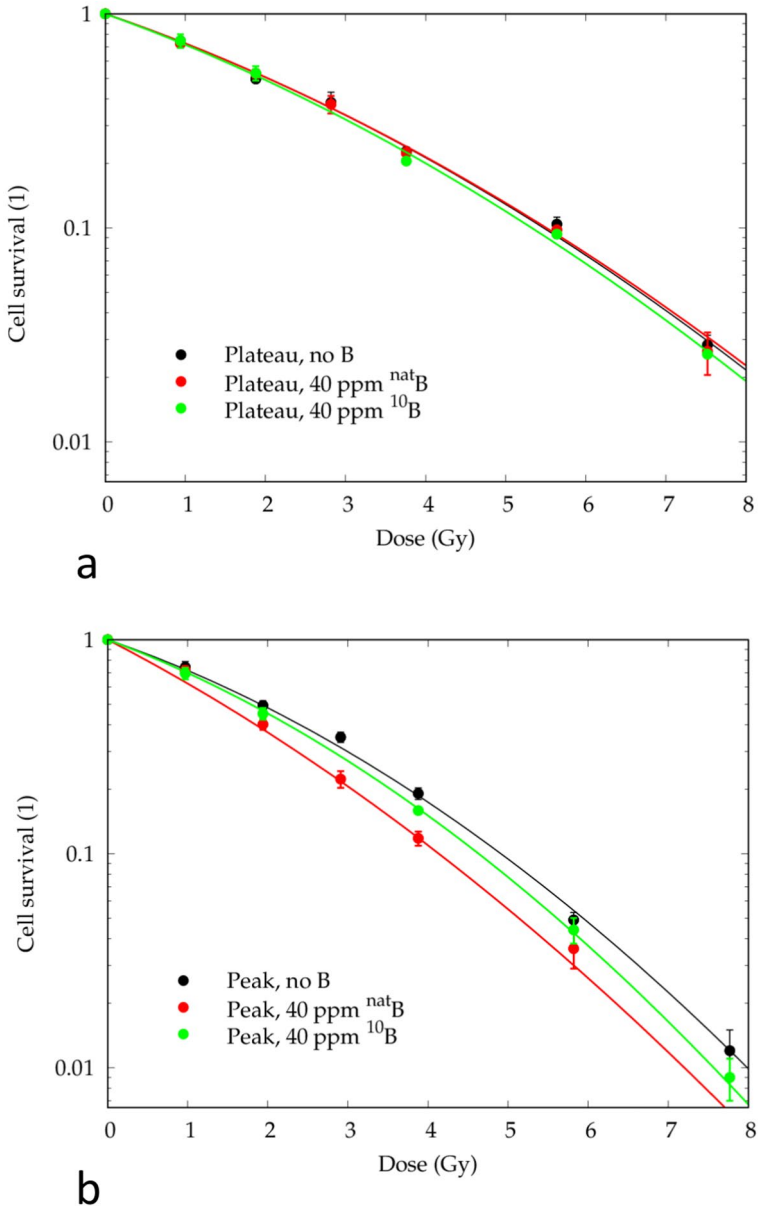


**Figure 2.** Survival of U-87 MG glioblastoma cells following irradiation by 190.6 MeV proton beams in (**a**) plateau or (**b**) peak regions without BSH (black) or with the presence of $^{nat}$BSH (red) or $^{10}$BSH (green) at a concentration of 40 ppm $^{nat}$B or $^{10}$B, respectively. Symbols represent mean values from at least 3 independent experiments, error bars depict standard errors of the mean, lines show linear-quadratic fits to the data.

| Position | Boron presence | α (Gy$^{-1}$) | β (Gy$^{-2}$) |
|---|---|---|---|
| Plateau | None | 0.295 ± 0.026 | 0.023 ± 0.004 |
| | $^{nat}$B | 0.297 ± 0.026 | 0.022 ± 0.004 |
| | $^{10}$B | 0.310 ± 0.037 | 0.023 ± 0.005 |
| Peak | None | 0.297 ± 0.028 | 0.035 ± 0.004 |
| | $^{nat}$B | 0.445 ± 0.058 | 0.027 ± 0.010 |
| | $^{10}$B | 0.321 ± 0.048 | 0.038 ± 0.006 |

**Table 2.** Coefficients α and β of the LQ fit to survival data for U-87 MG cells irradiated by 190.6 MeV protons under the presence or absence of 40 ppm $^{nat}$B or $^{10}$B in the form of BSH. Uncertainties are reported as standard deviations.

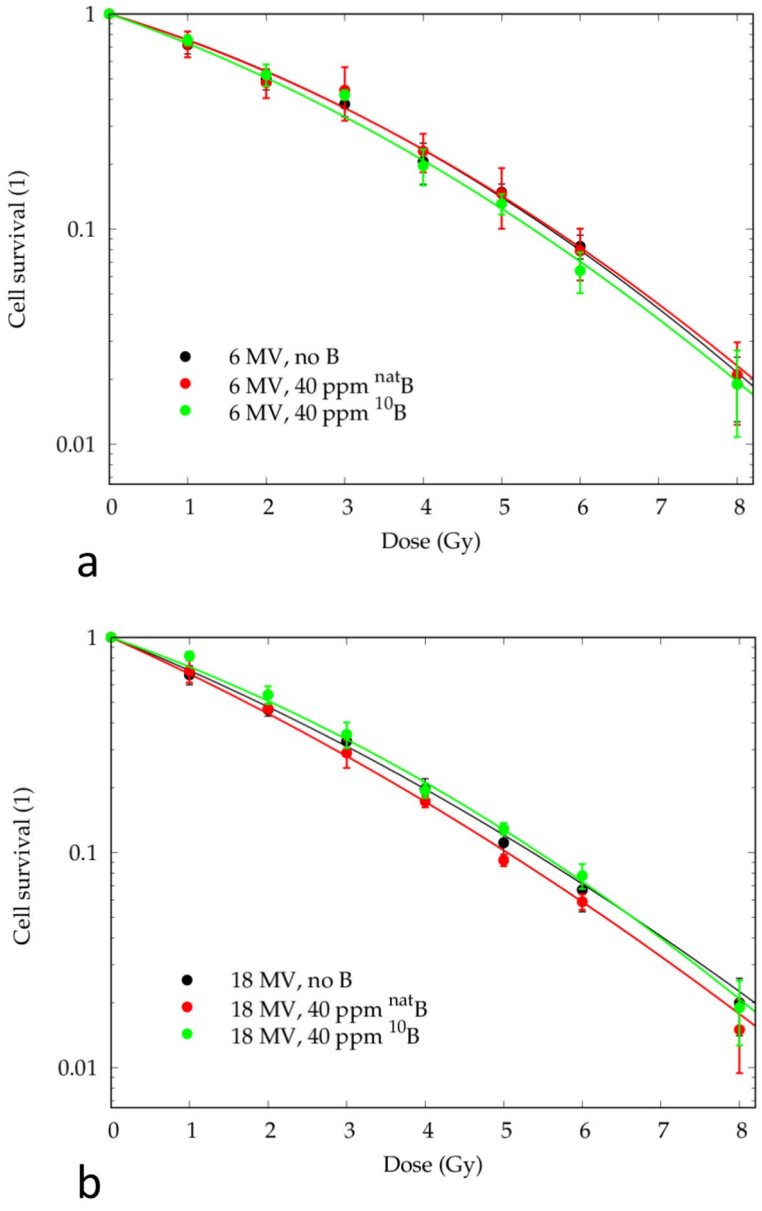


**Figure 3.** Survival of U-87 MG glioblastoma cells following irradiation by (**a**) 6 MV or (**b**) 18 MV photon beams without BSH (black) or with the presence of $^{nat}$BSH (red) or $^{10}$BSH (green) at a concentration of 40 ppm $^{nat}$B or $^{10}$B, respectively. Points represent mean values from 4 independent experiments, error bars depict standard errors of the mean, lines depict linear-quadratic fits to the data.

| Beam | Boron presence | α (Gy$^{-1}$) | β (Gy$^{-2}$) |
|---|---|---|---|
| 6 MV | None | 0.248 ± 0.048 | 0.029 ± 0.006 |
| | $^{nat}$B | 0.255 ± 0.062 | 0.027 ± 0.008 |
| | $^{10}$B | 0.292 ± 0.056 | 0.025 ± 0.008 |
| 18 MV | None | 0.338 ± 0.037 | 0.017 ± 0.005 |
| | $^{nat}$B | 0.376 ± 0.039 | 0.016 ± 0.005 |
| | $^{10}$B | 0.292 ± 0.043 | 0.024 ± 0.006 |

**Table 3.** Coefficients α and β of the LQ fit to survival data for U-87 MG cells irradiated by 6 or 18 MV photons under the presence or absence of 40 ppm $^{nat}$B or $^{10}$B in the form of BSH. Uncertainties are reported as standard deviations.

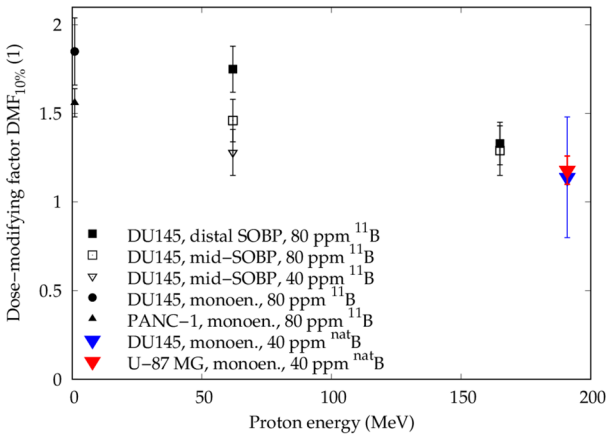


**Figure 4.** Dose-modifying factor at 10% cell survival $DMF_{10\%}$ for DU145 (blue) and U-87 MG cells (red) from the present study compared with values (black symbols) from pioneering PBCT experiments[3,5,6]. The legend items state the cell line, irradiation type, and concentrations of boron added in the form of BSH. Error bars represent standard deviations.

glioblastoma cell line, on which the present study was focused and for which correspondingly more experiments were performed, the enhancement was statistically highly significant ($p = 2 \times 10^{-5}$). For both cell lines, the presence of boron decreased cell survival after proton irradiation by about a factor of 2 at the highest doses studied, selectively in the Bragg peak region. At 10% cell survival, enhanced cell killing was observed as if the dose increased by about 14 or 18% for the studied cell lines. The reported results provide the first independent validation of PBCT in vitro and suggest it is not limited to a few cell lines but likely represents a rather general phenomenon.

Contrary to $^{nat}$BSH containing the natural boron isotopic mixture of 80% $^{11}$B and 20% $^{10}$B, there was little to no effect of $^{10}$BSH with virtually 100% $^{10}$B. Little to no modulations were observed for 6 or 18 MV photon beams with or without either form of BSH. Taken together, the results strongly suggest that the observed results are due to $^{11}$B, not due to other components of the BSH molecule such as sodium or the thiol group, and not due to $^{10}$B capturing secondary neutrons. The potential role of secondary neutrons could not have been excluded a priori but had to be assessed directly: Secondary neutrons including thermal as well as high-energy ones are known to be present in therapeutic proton fields, especially if the beams are spread out using passive modulation techniques but to a lesser extent also in active scanning techniques such as the one used in the present work[18,19]. The cross section for proton capture by $^{11}$B reaches about 1 b in a sharp peak around 0.7 MeV. The cross section of $^{10}$B for capturing thermal neutrons, 3840 b, may partially compensate for the several-orders-of-magnitude difference between secondary neutron and primary proton fluences, so that the number of boron-neutron capture events may become roughly comparable to that of proton-boron reactions. Also high-energy photon beams such as 18 MV ones used in this work contain considerable fluences of secondary neutrons. The performed dedicated experiments with $^{10}$BSH provided negative data, demonstrating that while neutron capture by $^{10}$B may contribute to the observed enhancement of cell killing by proton beams in the presence of $^{nat}$BSH, its role is clearly not dominant, at least for the studied U-87 MG cells. Further, the reported data provide no support for the previously suggested role of BSH acting as a general radiosensitizer[14]. The present data do not provide indication for a protective effect of the thiol (SH) group in the BSH molecule, either, contrary to observations in plasmid DNA[20].

Obviously, the reported data do not provide further insight into the underpinning mechanism regarding whether the key process is indeed the $p + {}^{11}B \rightarrow 3\alpha$ reaction. However, its involvement is consistent with the selectivity of PBCT to proton beams and their Bragg peak region, given the sharp maximum of the $p + {}^{11}B$ cross section at very low energies. The proton-boron capture reaction is a very rare event, occurring once per about a million of protons at clinically relevant boron levels as used here[10]. Being able to observe such rare events manifest at the cell population level implies that cells (or sub-cellular organelles such as mitochondria) are extremely sensitive radiation detectors. These initial events likely need to be amplified by neighbouring cells that did not directly participate in the interaction with the densely ionizing alpha particles. We have recently hypothesized that intercellular signalling is responsible for this amplification[21].

The present results extend the PBCT validity to high-energy (190 MeV) protons and boron levels as low as 32 ppm $^{11}$B (40 ppm $^{nat}$B). Both aspects are clinically relevant: High-energy beams are needed for irradiating deep-seated tumours; typically, clinical proton therapy centres are equipped with beam energies up to 250 MeV. While boron concentrations of 80–100 ppm can be reached in BNCT applications[8], having observed enhanced effectiveness at 32 ppm $^{11}$B (40 ppm $^{nat}$B) suggests PBCT is robust to potential issues with boron distribution in tissue e.g. due to a reduced blood perfusion.

The reported in vitro results demonstrated an enhanced effectiveness of proton beams in the Bragg peak region under the presence of boron not only for DU145 prostate cancer cells but also for U-87 MG cells derived from glioblastoma, an aggressive brain tumour. This suggests PBCT might increase the effectiveness of proton therapy for these tumours. This would be highly relevant, since glioblastomas are linked with expected patient survival of less than a year only[22]. Obviously, in vitro studies such as the present one are valuable in helping

elucidate the underpinning mechanisms, but it is up to preclinical and clinical studies to judge the validity of clinical methods in general and PBCT in particular. Importantly, in the period of preparing this manuscript, a pre-clinical study was published that used a xenograft model of glioblastoma generated by subcutaneously injecting U-87 MG cells to mice[23]. The authors reported enhanced cell killing, reduced metabolic tumour volume and total lesion glycolysis, as well as gene expression changes related to cellular communication, in line with the results reported in this work and supporting the potential clinical applicability of PBCT.

On the other hand, our own data[24] show large variations in the boron-mediated enhancement of proton effectiveness among cell lines, including the lack of enhancement in some cells at 40 or 80 ppm $^{nat}$B. This might be a consequence of the proposed key role of intercellular communication in the PBCT phenomenon: Radiation-induced signalling and its effects have been shown to depend on cellular characteristics, timing, and medium or serum composition including e.g. the presence of antioxidants or serotonin level[25,26]. Likely, variations in these factors may also help explain inconclusive or negative PBCT data reported in the literature[14–16]. The PBCT phenomenon, its underpinning mechanisms and potential clinical applications thus clearly deserve further research.

## Materials and methods

### Cell culture and boron treatment

Adherent DU145 prostate cancer cells (kindly provided by Prof. L. Manti, University of Naples, Italy) or U-87 MG human glioblastoma astrocytoma cells (ECACC) were used, as non-synchronized cell populations in their exponential phase. The cells were grown in tissue culture flasks (TPP, Techno Plastic Products AG, Trasadingen, Switzerland) in Minimum Essential Medium Eagle (MEME, Sigma-Aldrich, Germany) supplemented with 10% Fetal Bovine Serum (FBS, Biosera, France), 2 mM glutamine, 1% non-essential amino acids solution, 1 mM sodium pyruvate, 100 U/ml penicillin and 0.1 mg/ml streptomycin (all: Sigma-Aldrich, Germany) in an incubator maintained at 37°C in 5% $CO_2$ atmosphere. Under these culture conditions, the doubling time was approximately 30 h or 33 h and the plating efficiency 60 % or 20% for DU145 or U-87 MG cells, respectively.

The cells were seeded in tissue culture T25 flasks two days before irradiation at a concentration of 4000–10,000 cells/cm$^2$ in 4 ml media. One day before irradiation, 1 ml media without or with boron was added. As boron delivery agents, two forms of sodium mercaptododecaborate (BSH, mercapto-undecahydro-*closo*-dodecaborate, also called sodium borocaptate, $Na_2B_{12}H_{11}SH$): either $^{nat}$BSH with natural boron ($^{nat}$B) isotope ratio of 20% $^{10}$B and 80% $^{11}$B, or $^{10}$BSH with virtually 100% $^{10}$B (Katchem, Czech Republic). Stock BSH solution was prepared shortly before experiments by dissolving BSH in sterile distilled water. The final boron concentration in the total 5 ml media was 0.04 mg/ml $^{nat}$B or $^{10}$B, i.e. 40 ppm $^{nat}$B or $^{10}$B, corresponding to 0.083 mg/ml $^{nat}$BSH or 0.070 mg/ml $^{10}$BSH, respectively; control samples received no boron supplement.

### Irradiations

Proton irradiations were performed at the Proton Therapy Center Czech in Prague using monoenergetic irradiation maps of 190.6 MeV (range in water of 23.9 cm), covering an irradiation area of 20 cm × 20 cm at the isocentre using the pencil beam scanning mode with spot spacing of 4 mm. The gantry was positioned at 180°, irradiating the sample from below, through the patient couch. The cells with or without BSH were irradiated at two positions of the Bragg curve[27]. The first position was at 2.1 cm of water equivalent thickness (WET) corresponding to the plateau area (also called entrance region) with a dose-averaged linear energy transfer (LET) of 0.44 keV/µm; the second position at 23.6 cm WET corresponded to the Bragg peak area with a dose-averaged LET value of 3.11 keV/µm. The WET was adjusted using solid water (RW3) and polymethyl methacrylate slabs below the samples (Fig. 5a). The applied doses were calculated for both positions in the treatment planning system XiO (ELEKTA, Sweden) as done in the standard clinical routine at the facility. The calculated doses were benchmarked by a plane parallel ionization chamber (PPC05, IBA dosimetry, Belgium). The beam range was verified using a multi-layer ionization chamber ZEBRA (IBA Dosimetry, Belgium). Doses up to 8 Gy were applied (specifically, 0, 0.94, 1.88, 2.82, 3.76, 4.7, 5.64 and 7.52 Gy in the plateau position, and 0, 0.97, 1.94, 2.91, 3.88, 4.86, 5.82 and 7.77 Gy in the Bragg peak position; for simplicity, these doses are approximately referred to as 0, 1, 2, 3, 4, 6 and 8 Gy below). The dose uncertainty due to range or positioning errors was estimated not to exceed 2%.

All irradiations were repeated several times using independent cell cultures. For DU145 cells, two independent repeats were performed measuring survival curves (methodology described below) by irradiating the cells with 0, 1, 2, 3 and 4 Gy, and then further two repeats with the dose range extended to 5 or 6 Gy in the peak or plateau positions, respectively, so that in total there were 2–4 independent repeats per datum. For U-87 MG cells, three repeats were performed with 0, 1, 2, 3 and 4 Gy without or with $^{nat}$B, followed by four repeats with doses up to 8 Gy without or with $^{nat}$B or $^{10}$B (only 3 repeats with $^{10}$B in plateau position), providing in total 3–7 independent repeats per datum. Here, 'datum' includes dose level, absence or presence of 40 ppm $^{nat}$B or $^{10}$B, and plateau or peak positions.

Photon irradiations were performed at the Thomayer University Hospital in Prague using linac (Siemens ARTISTE, Germany) photon beams of 6 or 18 MV. For both energies, the source-to-axis distance was 90 cm and the irradiation field size was 20 cm × 20 cm at the isocentre. The delivered doses were determined using the treatment planning system XiO by ELEKTA as done in routine clinical operation of the machine. The dose delivery uncertainty was 0.5%, estimated from previous dosimetric assessments. Samples were positioned horizontally on the treatment couch. Solid water slabs were used to assure the dose rate of 2 Gy/min. The gantry was positioned at 180°, irradiating the sample from below, through the patient couch. Additional solid water slabs were placed above the sample to include backscattered radiation. Doses up to 8 Gy were applied. The irradiation scheme and the percentage depth-dose curves for the used beams are shown in Fig. 5b. All irradiations were repeated four times using independent cell cultures.

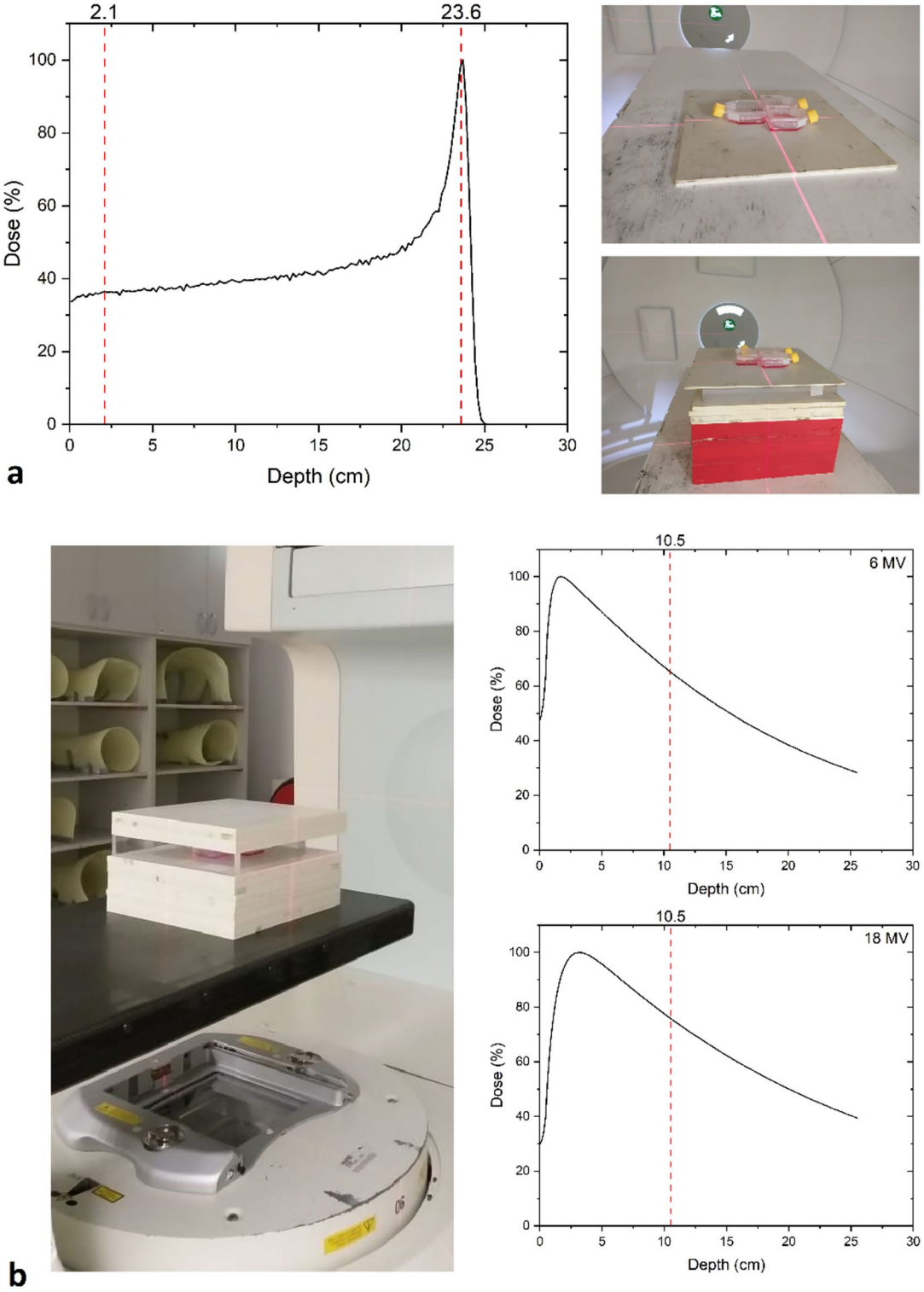


**Figure 5.** (**a**) Proton irradiations. Left: Percentage depth-dose curve, acquired using a ZEBRA multi-layer ion chamber device, with marked irradiation positions of 2.1 cm (plateau) and 23.6 cm (Bragg peak). Right: Experimental setup at the Proton Therapy Center Czech in Prague. The samples were irradiated from below. The depth was realized using slabs in both plateau (top) and peak regions (bottom). (**b**) Photon irradiations. Left: Experimental setup using Siemens ARTISTE linac. The samples were irradiated from below. Right: Percentage depth-dose curves with marked irradiation positions for 6 MV (top) and 18 MV photon beams (bottom).

### Cell incubation and clonogenic cell survival assay

Immediately after returning from the irradiation facilities, the cells were washed twice by 1X Phosphate Buffered Saline (Sigma-Aldrich, Germany) and trypsinized using 1X Trypsin–EDTA (Biosera, France) for 3 min in the incubator. Then 4 ml of medium were added, and cell concentrations were counted by a MUSE cell analyzer (EMD Millipore) using the Muse Count & Viability Assay Kit (Merck Millipore/Luminex, MCH100102) according to the manufacturer's instructions. Cells were then re-seeded to 6-well plates (providing 6 technical replicates per datum and repeat) with fresh, boron-free medium at appropriate densities estimated to yield about 30 colonies per well, given the expected survival levels. Following incubation for 12 days at 37°C in 5% $CO_2$ atmosphere, the formed colonies were fixed and stained using Crystal violet dye (Sigma-Aldrich, Germany) diluted in water and methanol. The colonies were counted manually, considering only those containing at least 50 cells. Cell survival fraction SF(D) at dose D was calculated as the ratio of plating efficiencies PE(D) at this dose and PE(0) in unirradiated controls, the PE being given by the ratio of the number of colonies observed to the number of cells seeded.

### Statistical analysis of survival data

Cell survival fraction (SF) in dependence on applied dose (D) was fitted by the Linear-Quadratic (LQ) model, $SF = \exp(-(\alpha D + \beta D^2))$, with parameters α and β, using the maximum likelihood fitting for Poisson-distributed data implemented in CFAssay tool[28]. In this step, the total number of cells seeded and colonies scored in the 6 replicates (6 wells of a plate) were considered, for each irradiation type (plateau or peak position for protons, or 6 or 18 MV photons), boron level (controls without boron or samples with $^{nat}B$ or $^{10}B$) and dose level. Each experiment was independently repeated several times as specified above. Statistical significance of the observed differences for pairs of survival curves, in particular those with versus without the presence of boron, was assessed by ANOVA-based tests for one-way designs in CFAssay[28]. The number of repeats per datum was reflected in its uncertainty (presented by error bars in the survival plots) as well as in the statistical power of differences between curves (p-values) estimated by CFAssay.

Dose modifying factor (DMF) of boron was calculated as the ratio of doses without versus with boron presence, for protons in the Bragg peak and 10% survival level, chosen throughout this work for consistency with the literature[3,5,6]. The doses leading to 10% survival were estimated from LQ fits to the data. Standard error propagation techniques were used to estimate uncertainties in the DMF from those of the LQ parameters.

## Data availability

The datasets generated and analysed during the current study are available from the corresponding author on reasonable request.

Received: 28 April 2024; Accepted: 5 August 2024
Published online: 20 August 2024

## References

1. Mohan, R. & Grosshans, D. Proton therapy—Present and future. *Adv. Drug Deliv. Rev.* **109**, 26–44. https://doi.org/10.1016/j.addr.2016.11.006 (2017).
2. Yoon, D. K., Jung, J. Y. & Suh, T. S. Application of proton boron fusion reaction to radiation therapy: A Monte Carlo simulation study. *Appl. Phys. Lett.* **105**, 223507. https://doi.org/10.1063/1.4903345 (2014).
3. Cirrone, G. A. P. *et al.* First experimental proof of proton boron capture therapy (PBCT) to enhance protontherapy effectiveness. *Sci. Rep.* **8**, 1141. https://doi.org/10.1038/s41598-018-19258-5 (2018).
4. Monti Hughes, A. & Hu, N. Optimizing boron neutron capture therapy (BNCT) to treat cancer: An updated review on the latest developments on boron compounds and strategies. *Cancers* **15**, 4091. https://doi.org/10.3390/cancers15164091 (2023).
5. Bláha, P. *et al.* The proton-boron reaction increases the radiobiological effectiveness of clinical low- and high-energy proton beams: Novel experimental evidence and perspectives. *Front Oncol.* **11**, 682647. https://doi.org/10.3389/fonc.2021.682647 (2021).
6. Ricciardi, V. *et al.* A new low-energy proton irradiation facility to unveil the mechanistic basis of the proton-boron capture therapy approach. *Appl. Sci.* **11**, 11986. https://doi.org/10.3390/app112411986 (2021).
7. Barth, R. F., Mi, P. & Yang, W. Boron delivery agents for neutron capture therapy of cancer. *Cancer Commun.* **38**, 35. https://doi.org/10.1186/s40880-018-0299-7 (2018).
8. Hideghéty, K. *et al.* 11Boron delivery agents for boron proton-capture enhanced proton therapy. *Anticancer Res.* **39**, 2265–2276. https://doi.org/10.21873/anticanres.13343 (2019).
9. Jung, J. Y. *et al.* Comparison between proton boron fusion therapy (PBFT) and boron neutron capture therapy (BNCT): A Monte Carlo study. *Oncotarget* **8**, 39774–39781. https://doi.org/10.18632/oncotarget.15700 (2017).
10. Mazzone, A., Finocchiaro, P., Lo Meo, S. & Colonna, N. On the (un)effectiveness of proton boron capture in proton therapy. *Eur. Phys. J. Plus* **134**, 361. https://doi.org/10.1140/epjp/i2019-12725-8 (2019).
11. Tabbakh, F. & Hosmane, N. S. Enhancement of radiation effectiveness in proton therapy: Comparison between fusion and fission methods and further approaches. *Sci. Rep.* **10**, 5466. https://doi.org/10.1038/s41598-020-62268-5 (2020).
12. Meyer, H. J., Titt, U. & Mohan, R. Technical note: Monte Carlo study of the mechanism of proton-boron fusion therapy. *Med. Phys.* **49**, 579–582. https://doi.org/10.1002/mp.15381 (2022).
13. Safavi-Naeini, M. *et al.* Opportunistic dose amplification for proton and carbon ion therapy via capture of internally generated thermal neutrons. *Sci. Rep.* **8**, 16257. https://doi.org/10.1038/s41598-018-34643-w (2018).
14. Manandhar, M. *et al.* Effect of boron compounds on the biological effectiveness of proton therapy. *Med. Phys.* **49**, 6098–6109. https://doi.org/10.1002/mp.15824 (2022).
15. Hosobuchi, M. *et al.* Experimental verification of efficacy of pBCT in terms of physical and biological aspects. *Nucl. Instrum. Methods Phys. Res. A* **1045**, 167537. https://doi.org/10.1016/j.nima.2022.167537 (2023).
16. Shtam, T. *et al.* Experimental validation of proton boron capture therapy for glioma cells. *Sci. Rep.* **13**, 1341. https://doi.org/10.1038/s41598-023-28428-z (2023).
17. Naseri, A. & Mesbahi, A. A review on photoneutrons characteristics in radiation therapy with high-energy photon beams. *Rep. Pract. Oncol. Radiother.* **15**, 138–144. https://doi.org/10.1016/j.rpor.2010.08.003 (2010).

18. Hälg, R. A. & Schneider, U. Neutron dose and its measurement in proton therapy—Current state of knowledge. *Br. J. Radiol.* **93**, 20190412. https://doi.org/10.1259/bjr.20190412 (2020).
19. Stolarczyk, L. *et al.* Dose distribution of secondary radiation in a water phantom for a proton pencil beam-EURADOS WG9 intercomparison exercise. *Phys. Med. Biol.* **63**, 085017. https://doi.org/10.1088/1361-6560/aab469 (2018).
20. Jamborová, Z. *et al.* Radiation damage to DNA plasmids in the presence of borocaptates. *Radiat. Prot. Dosim.* **198**, 532–536. https://doi.org/10.1093/rpd/ncac094 (2022).
21. Kundrát, P. *et al.* Boron-enhanced biological effectiveness of proton irradiation: Strategy to assess the underpinning mechanism. *Radiat. Prot. Dosim.* **198**, 527–531. https://doi.org/10.1093/rpd/ncac093 (2022).
22. Brown, N. F. *et al.* Survival outcomes and prognostic factors in glioblastoma. *Cancers* **14**, 3161. https://doi.org/10.3390/cancers14133161 (2022).
23. Cammarata, F. P. *et al.* Proton boron capture therapy (PBCT) induces cell death and mitophagy in a heterotopic glioblastoma model. *Commun. Biol.* **6**, 388. https://doi.org/10.1038/s42003-023-04770-w (2023).
24. Jelínek Michaelidesová, A. *et al.* Variations among glioblastoma cell lines in boron-mediated enhancement of cell killing by proton beams. In preparation (2024).
25. Prise, K. M. & O'Sullivan, J. M. Radiation-induced bystander signalling in cancer therapy. *Nat. Rev. Cancer* **9**, 351–360. https://doi.org/10.1038/nrc2603 (2009).
26. Mothersill, C., Saroya, R., Smith, R. W., Singh, H. & Seymour, C. B. Serum serotonin levels determine the magnitude and type of bystander effects in medium transfer experiments. *Radiat. Res.* **174**, 119–123. https://doi.org/10.1667/RR2036.1 (2010).
27. Michaelidesová, A. *et al.* In vitro comparison of passive and active clinical proton beams. *Int. J. Mol. Sci.* **21**, 1–15. https://doi.org/10.3390/ijms21165650 (2020).
28. Braselmann, H., Michna, A., Heß, J. & Unger, K. CFAssay: Statistical analysis of the colony formation assay. *Radiat. Oncol.* **10**, 223. https://doi.org/10.1186/s13014-015-0529-y (2015).


## Author contributions

Conceptualization, Ma.D., V.V., P.K. and A.J.M.; methodology, Ma.D. and A.J.M.; investigation, A.J.M., Ma.D., O.Z., J.Va., K.P.B., I.D., J.Vi. and Mi.D.; data analysis, A.J.M. and P.K.; writing- original draft preparation, P.K. and A.J.M.; all authors have read and agreed to the published version of the manuscript.


## Funding

This research was funded by the Czech Science Foundation, project number 21-06451S.


## Competing interests

The authors declare no competing interests.

## Additional information

**Correspondence** and requests for materials should be addressed to M.D.

**Reprints and permissions information** is available at www.nature.com/reprints.

**Publisher's note** Springer Nature remains neutral with regard to jurisdictional claims in published maps and institutional affiliations.